Feature Points Matching of Nonrigid Tissues Based on SURF, Spatial Association Correspondence and Clustering: Application to MR 2-D Slice Deformation Measurement

Xubing Zhang [1,2], Shinichi Hirai [1], Penglin Zhang[3]
[1]Dept. of Robotics, Faculty of Science and Engineering, Ritsumeikan University, Kusatsu, Shiga 525-8577, Japan
[2]School of Computer Science, Wuhan Textile University, Wuhan 430073, China
[3]School of Remote Sensing and Information Engineering, Wuhan University, Wuhan 430079,China

***Abstract*-Due to the nonlinear and nonuniform local deformation of the nonrigid tissues, it is difficult whereas important to extract and correctly match a considerable number of feature points from the MR images for deformation measurement. Current approaches are dissatisfying towards this issue. In this paper, firstly the authors use SURF algorithm to extract the feature points in the initial MR image, and take every point in the deformed MR image as the feature point. Then the SURF descriptors and Spatial Association Correspondence (SAC) of the neighborhood pixels is adopted to match the corresponding feature points between the initial and deformed MR images. Finally, by clustering the coordinate differences between the deformed points matched by SURF-SAC with the corresponding points calculated by affine transformation, most of wrong match points are eliminated. The experimental results prove that the proposed method can extract and match more correct corresponding feature point pairs than SURF and SIFT methods.**

***Key words*—SURF, Spatial Association Correspondence, Clustering, Feature point, Matching, Deformation**

I. INTRODUCTION

Deformation field measurement of nonrigid biological tissues from MR (Magnetic Resonance) images is often required for clinical diagnosis, surgery simulation, operation planning, and evaluation of physical characteristics of biological tissues [1-4]. Usually we need to measure the local irregular deformations accurately between the two MR images obtained at different rotation, displacement, and soft tissue deformations. In our opinions, current nonrigid medical image registration and deformation measurement methods can be classified into four categories, transformation model estimation [5-7], physical model method [8-12], mutual information [13-14], and feature points combined with TIN (Triangular Irregular Network) [1-2].

The space transformation model such as low degree polynomial [5], thin plate splines (TPS) [6], and B-splines [7] can be applied to measure the nonlinear deformation of images. According to such approaches, the interpolation and matching of images is based on many feature points. Actually, it is difficult to extract and correctly matched a considerable number of feature points between the deformed images.

The typical methods of physical model include elastic deformation model [8-9], viscous fluid [10], optical flow [11], and finite element [12]. In elastic deformation models, popular parametric deformation model cannot handle topological changes [8], and geometric active model cannot measure the interior deformation and tends to leak through the weak boundary [9]. The viscous fluid method tends to wrong matching when there are some different tissue fabrics with similar pixel intensity distribution. When the gradient information is weak, the optical flow method cannot behave well in the deformation image estimation. The deformation measurement accuracy of finite element model depends on the matching boundary of image fabric, which is difficult to obtain.

The maximal mutual information method is originally applied in the rigid image registration. Now it is widely adopted to match the nonrigid deformed images when combined with the other methods, such as thin-plate splines, B-splines, optical model and so on. In these cases, the mutual information method mainly acts as a global estimate of the image registration accuracy, so that it cannot avoid the limitation of the other combined methods.

Zhang presented a deformation field measurement method based on the feature point tracking and Delaunay TIN. Considering the irregular local deformation of nonrigid and nonuniform tissues, Zhang extracts and matches a considerable number of feature points in MR images by means of Harris algorithm and relaxation labeling method, and then the Delaunay TIN is constructed based on feature points to measure the deformation fields. While in this method, the initial rough match is based on the points around the rigid bone, and actually, a certain number of wrong matched points which have negative effect on measurement accuracy cannot be eliminated automatically [1], [2].

According to above discussion, we can see that the extraction and correct matching of a considerable number of feature points is very important to the deformation measurement of nonrigid biological tissues, also it is a key difficult to be solved.

Extraction and matching of the feature points, which should be robust against the change in illumination, scaling, rotation, and noise or slight distortion, is one of the most important methods used to detect the correspondences between the images. A wide variety key point detectors and descriptors have already been proposed in the literature [15-18]. The most widely used detector probably is the Harris corner detector [19], based on the eigenvalues of the second-moment matrix. However, Harris corners are not scale-invariant. Lindeberg introduced the concept of automatic scale selection, which detects interest points with their own characteristic scale [15]. Mikolajczyk and Schmid created robust and scale-invariant feature detectors with high repeatability, called Harris-Laplace and Hessian-Laplace [20].

Lowe presented the Scale Invariant Feature Transform (SIFT) approach, which approximated the Laplacian of Gaussian (LoG) by a Difference of Gaussians (DoG) filter [16], and can bring speed at a low cost in terms of lost accuracy [21], [22]. Shown in the literature [22], SIFT outperforms the other feature descriptors like Gaussian derivatives [23], moment invariants [24], complex features [25], phase-based local features. Various refinements on the SIFT scheme have been proposed, the PCA-SIFT and the GLOH methods are known well in them [18], [22].

Bay Herbert presented SURF (Speeded-UP Robust Feature) in 2006 [26], it is invariant to scaling, rotating, illumination change, affine transformation, and is robust to noise and detection errors. By using the 'Fast-Hessian' to approximate the Laplacian, describing a distribution of Haar-wavelet responses within the interest point neighborhood, reducing the descriptor to 64 dimensions, and exploiting integral images, the SURF is more repeatable, distinctive, robust, and furthermore the computing velocity is three times more than SIFT. In the experimental results, Bay also proved that, SURF outperformed the other methods such as GLOH and PCA-SIFT [22], [26], [27].

Unfortunately, when we attempted to evaluate the deformation measurement by SURF, the experimental results were not inspiring. The amount of the matched points was too few and not enough to construct the TIN which was very important to the accurate deformation measurement.

In order to obtain more correct matched points, the authors combined the SURF with the analysis of spatial association correspondence to extract and match the feature points between the initial and deformed MR images. Secondly, in order to eliminate the wrong matched point pairs, we apply clustering to analyze the coordinate differences between the deformed corresponding points matched by our method and the theoretic corresponding points calculated by the affine transformation. The points which are not included in the range of the maximum clustering are regarded as the wrong matching points.

In our experiments, the SIFT, SURF, and the method combined SURF, SAC and clustering are compared, and the results showed that SURF-SAC can obtain more correct corresponding points, furthermore, most of wrong matching feature points can be eliminated by adopting coordinate difference clustering algorithm.

II. SURF

The interest point detector of SURF is based on the Hessian matrix. It relies on integral images to reduce the computation time and called 'Fast-Hessian' detector [20]. On the other hand, the descriptor of interest point describes a distribution of Haar-wavelet responses within the interest point neighbourhood.

A. Fast-Hessian Detector

Rather than using a different measure for selecting the location and the scale as the Hessian-Laplace detector [20], SURF relies on the determinant of Hessian for both. Given a point $p = (x, y)$ in an image *I*, the Hessian matrix $\mathrm{H}(p,\sigma)$ in *P* at scale σ is defined as follows

$$H(p,\sigma) = \begin{bmatrix} L_{x,x}(p,\sigma) & L_{x,y}(p,\sigma) \\ L_{x,y}(p,\sigma) & L_{y,y}(p,\sigma) \end{bmatrix}, \qquad (1)$$

where σ is the scale factor, $L_{x,x}(p, \sigma)$ is the convolution of Gaussian second order derivative $(\partial^2 / \partial x^2) g(\sigma)$ with the image *I* in point *p*, and similarly for $L_{x,y}(p, \sigma)$ and $L_{y,y}(p, \sigma)$.

As Gaussian filters are nonideal in any case, and given Lowe's success with LoG approximations, Bay further applied the box filters to approximate the second order Gaussian derivatives. The other hand, the integral images is applied to accelerate the process of interested point detection and descriptor estimation, independently of the image size. The 9×9 box filters $D_{x,x}$, $D_{x,y}$ and $D_{y,y}$ in Fig. 1 approximate Gaussian second order derivatives with the lowest scale σ = 1.2, and the grey regions in the figures equal to zero.

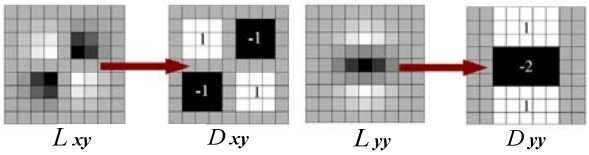

Figure 1. The box filters Dx,y and Dy,y used to approximate Gaussian second order partial derivatives in xy-direction and yy-direction

The weights, 1 in black regions while –1 in white regions, applied to the rectangular regions are kept simple for computational efficiency. Bay proposes the following formula as an accurate approximation for the Hessian determinant using the approximated Gaussians:

$$\det(H_{approx}) = D_{xx}D_{yy} - (0.9D_{xy})^2 \qquad (2)$$

In SURF, the scale space can be created by applying kernels of increasing size to the original image. This allows multiple layers of the scale space pyramid to be processed

simultaneously. The scale-space is divided into a number of octaves, where an octave refers to a series of response map layers covering a doubling of scale. In SURF the output of the above 9×9 filter is considered as the lowest level of scale space, which correspond to a real valued Gaussian with σ = 1.2. The scales of subsequent layers can be evaluated by the following formula

$$\sigma_{approx} = CurrentFilterSize \cdot (1.2/9). \quad (3)$$

In the lowest octave, the filter size of the first layer is 9×9, and the filter size increases by 6 between the two neighboring layers. For each new octave, the filter size increases double.

B. Descriptor

The SURF descriptor describes how the pixel intensities are distributed within a scale dependent neighbourhood of each interest point detected by the Fast-Hessian. This approach is similar to that of SIFT but integral images used in conjunction with filters known as Haar wavelets are used in order to increase robustness and decrease computation time. The first step consists of fixing a reproducible orientation based on information from a circular region around the interest point. Then describing the interest point by calculating the Haar wavelet responses over the square region aligned to the selected orientation.

1) Orientation Assignment: Assigning the interest point a reproducible orientation is to achieve invariance to image rotation. To determine the orientation, Haar wavelet responses of size 4σ are calculated for a set of pixels around the detected point with a radius of 6σ, where σ refers to scale at which the point was detected.

Once the wavelet responses are weighted with a Gaussian (2.5σ) centered at the interest point, they are represented as vectors in space with the horizontal response strength along the abscissa and the vertical response strength along the ordinate. The dominant orientation is estimated by calculating the sum of all responses within a sliding orientation window covering an angle of $\pi/3$. The longest responses vector lends its orientation to the interest point.

2) Descriptor Components: The first step in extracting the SURF descriptor is to construct a square window around the interest point. This window contains the pixels which will form entries in the descriptor vector and is of size 20σ, where σ also refers to the detected scale. Furthermore the window is oriented along the dominant orientation such that all subsequent calculations are relative to this direction.

As shown in Fig. 2 the descriptor window is divided into 4 ×4 regular subregions. Within each subregion Haar wavelets of size 2σ are calculated for 25 regularly distributed sample points. If we refer to the *x* and *y* wavelet responses by *dx* and *dy* respectively, then for these 25 sample points (i.e. each subregion) we collect,

$$v_{subregion} = \left[\sum dx, \sum dy, \sum |dx|, \sum |dy|\right]. \quad (4)$$

Therefore each subregion contributes four values to the descriptor vector leading to an overall vector of length 4×4 × 4 = 64. The resulting SURF descriptor is invariant to rotation, scale, brightness and, after reduction to unit length, contrast.

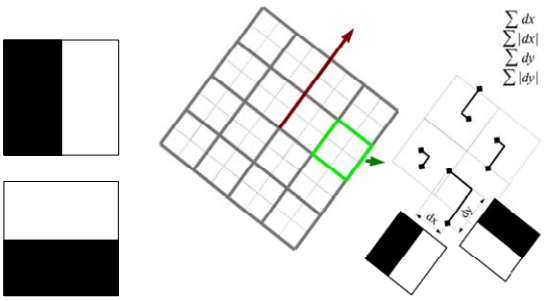

Figure 2. Left: Haar wavelet types for SURF (top the x-direction and bottom the y-direction). Right: SURF descriptor component. The brown arrow directs the dominant orientation, and the green rectangle refers to one of the descriptor subregion.

III. Spatial Association Correspondence

Although SURF is outstanding to extract the invariant interest points in an image, the number of correctly matched point pairs is too few to measure the tissue deformation accurately. Actually, many interest points that SURF extracts between the initial and deformed images are not really corresponding because of the nonuniform elastic deformation of the nonrigid tissues. In this paper the Spatial Association Corresponding method is proposed to obtain more correctly matched point pairs.

A. Spatial Association Correspondence

The Spatial Association Correspondence method is based on the supposition that the neighboring pixels in the initial MR image would also be most probably neighboring in the deformed MR image although the elastic deformation.

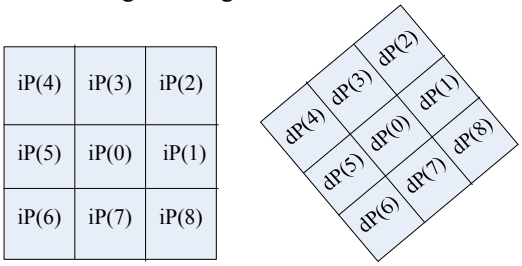

Figure 3. A pair of corresponding pixel neighbourhood regions between initial and deformed MR images. Left: neighbourhood in initial image, Right: corresponding neighbourhood in deformed image.

As shown in Fig. 3, there is a pixel neighbourhood region in initial and deformed image respectively. Because the pixel neighborhood has only 9 pixels and is very small, we only need consider the rotation and translation. We can suppose that if the initial point *iP(0)* is corresponding to the deformed point *dP(0)*, the initial neighboring pixel *iP(1)* would be corresponding to the deformed neighborhood pixel *dP(1)*.

Pixels *iP(2)* through *iP(8)* also correspond to the *dP(2)* though *dP(8)*.

B. *Feature Point Matching*

How to match the interest points between the images is based on the method as follows:

iP(0)	dP(0_1)	dP(0_2)	dP(0_3)	……	dP(0_k0)
iP(1)	dP(1_1)	dP(1_2)	dP(1_3)	……	dP(1_k1)
iP(2)	dP(2_1)	dP(2_2)	dP(2_3)	……	dP(2_k2)
⋮					
iP(8)	dP(8_1)	dP(8_2)	dP(8_3)	……	dP(8_k8)

Figure 4. Candidate corresponding points of the the neighbourhood of *iP(0)*.

1) Corresponding Candidates Searching: We extract and match several correctly corresponding point pairs between the two images by means of SURF and the ratio of the nearest and the second nearest neighbor (NN/SCN) matching method. Then approximate affine transformation model of deformed image is calculated with the several matching pairs.

For the interest point *iP(0)* extracted, we only need to search a region in the deformed image. This region centered with the corresponding point of *iP(0)* calculated by the approximate affine transformation model, and the range of the corresponding region reflects a pre-estimation of maximum deformation. The SURF descriptors distances between *iP(0)* and all of the pixels in the corresponding region are compared. Usually, the point with the least descriptor distance to *iP(0)* may not be the real corresponding point. So we can set a threshold which is a little bigger than the least descriptor distance to *iP(0)*, the deformed pixels whose SURF descriptor distances to *iP(0)* are smaller than the threshold will be taken as the corresponding candidates such as *dP(0_1)* through *dP(0_k0)*. For the other pixels in the 3×3 neighborhood of pixel *iP(0)*, the corresponding candidates would be detected by the same process. For every point of *iP(0)* through *iP(8)* there are several corresponding candidates in the deformed image as shown in Fig. 4.

2) Corresponding Point Detection: In this step, we need to detect the corresponding point of *iP(0)* from the corresponding candidates by using Spatial Association Corresponding as shown in Fig. 5.

Firstly, we create a chain set *C*, which consists of the corresponding candidates of *iP(0)*, those are *dP(0_1)* through *dP(0_k0)*, as shown in the Fig. 5-a) are the red circles. Secondly, if every corresponding candidate of *iP(1)*, which refers to the green circle, is adjacent to any corresponding candidates of *iP(0)*, the two candidates are composed as a new binary chain element of the chain set *C*. Then check the set *C*, and eliminate the elements which consist of only one point, Such as the {*dP(0_4)*} and {*dP(0_6)*} in Fig. 5-b). Thirdly, if every corresponding candidate of *iP(2)*, which refers to the blue circle, is adjacent with both of the corresponding candidates of *iP(0)* and *iP(1)* in one of the binary chain elements of *C*, and the spatial position relationship between the three candidates is the same as *iP(0)*, *iP(1)* and *iP(2)* except the rotation, it is combined with the binary chain as a ternary chain element of *C*. Similarly eliminate the elements which consist of only two point, such as the {*dP(0_5)*, *dP(1_5)*} in Fig. 5-c).

Step by step, we check the corresponding candidate points of the other neighboring points *iP(3)* through *iP(8)* as the same process shown above. When only one element left in the chain set, we regard the first point of the element as the corresponding point of the pixel *iP(0)*.

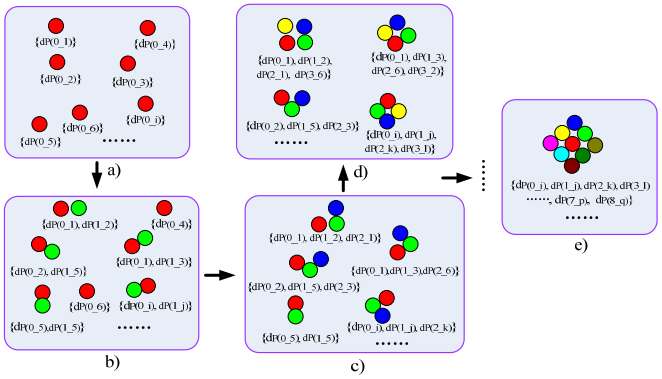

Figure 5. Corresponding point detection process of *iP(0)*.

IV. CLUSTERING

Actually, although matching the points between the initial and deformed images by means of the SURF and Spatial Association Correspondence, many feature points are incorrectly matched because of the deformation, blurry, noise, or other complex influence factors of the MR images. In order to eliminate the wrong matching points, the authors adopt the affine transformation and the clustering of the coordinate differences between the corresponding points matched by our method and the corresponding points calculated by the affine transformation method.

A. *Affine Transformation*

Given a point *P* in the initial image, the corresponding point *P'* in the deformed image matched by the affine transformation is as follows

$$p' = p \cdot T_{affine}, \tag{5}$$

where T_{affine} is the affine transformation matrix, which can be calculate by

$$T_{afine} = T_{scale} \times T_{rotate} \times T_{trans}, \quad (6)$$

where T_{scale}, T_{rotate} and T_{trans} are respectively scaling matrix, rotate matrix and translation motion matrix, given as follows:

$$T_{scale} = \begin{bmatrix} u & 0 & 0 \\ 0 & v & 0 \\ 0 & 0 & 0 \end{bmatrix}, \quad (7)$$

$$T_{rotate} = \begin{bmatrix} \cos\theta & \sin\theta & 0 \\ -\sin\theta & \cos\theta & 0 \\ 0 & 0 & 1 \end{bmatrix}, \quad (8)$$

$$T_{trans} = \begin{bmatrix} 1 & 0 & \Delta x \\ 0 & 0 & \Delta y \\ 0 & 0 & 1 \end{bmatrix}. \quad (9)$$

There are five variables in the three matrices; the scaling parameter u and v are along x-direction and y-direction respectively, θ is the rotation angle, Δx and Δy are the displacement along x-direction and y-direction.

B. Difference Clustering

In this paper, several correct matched pairs of points are detected by SURF, and the affine transformation was evaluated based on the least square method. Then, the difference cluster method is adopted to judge a pair of matching points is correctly corresponding or not.

The difference clustering is as follows. Suppose that $P(x, y)$ refers to a feature point in the initial image, $P'(x', y')$ is the corresponding point in the deformed image calculated by the affine transformation T_{affine}, and $P''(x'', y'')$ is the corresponding point in the deformed image matched by SURF-SAC. The difference between P' and P'' refers to difference point $dP(d_x, d_y)$ is as follows

$$dp(d_x, d_y) = (p'' - p') = \begin{bmatrix} x'' \\ y'' \end{bmatrix} - \begin{bmatrix} x' \\ y' \end{bmatrix}. \quad (10)$$

Difference clustering method is based on the supposition that if the point pairs are matched correctly the values of their difference points maybe most probably near to each other. Because the main tendencies of the biological deformation in the correct matched points are probably similar to each other, although the deformation displacements of them are not uniform. The other hand, the wrong matched point elimination is based on our method SURF-SAC, and the affine transformation can evaluate the great deformation such as scaling, rotation, and translation.

Given R refers to the cluster radius, $C(i)$ refers to a cluster centered with the difference point $dP(i)$, and $C(i)$ consists of the difference points whose distance with $dP(i)$ is less than R. In this paper, every difference point is taken as the cluster center, and the cluster which includes the most difference points are considered as consisting of correctly matched feature points.

V. Experiment Results Analysis

In our experiments, SIFT, SURF, and the proposed SURF-SAC are compared. An initial MR 2-D slice image and a deformed MR 2-D slice image of the volunteer's calf are tested. For SIFT and SURF method, the image pyramid consists of 3 octaves, every octave have 4 layers with the different scales (more octaves and more layers are not better to this experiments), and after the feature points are extracted, the method of NN/SCN is adopted to match the feature points between MR images. The procedure of SURF-SAC is as follows. 1) Extract the feature points in the initial MR image by SURF; 2) Take all the points in the deformed MR image as the feature points, and match the feature points between the two images based on SURF-SAC; 3) Eliminate the wrong matched pairs by coordinate difference clustering. We showed the experiments results from Fig. 6 to Fig.10.

The experiment results of SIFT were shown in Fig. 6. We can see that only 9 pairs of points are matched, which were signed in Fig. 6-b). Furthermore, the pairs 7 and 9 are matched incorrectly obviously.

The experiment results of SURF were shown as Fig. 7. The parameter T is defined as the threshold value of the determinant of the Fast-Hessian, the point whose fast-Hessian determinant is smaller than T would not be extracted. We set T equal to 0.0004. In SURF experiments, among many feature points extracted by SURF, there are 41 pairs of points are matched, even though the ratio of NN/SCN is assigned to 0.9 to obtain more matched pairs. Furthermore only 11 pairs of points are matched correctly, and the matching correct rate is 26.83%.

The experiment results of SIFT and SURF showed that the correct matched points was few, which are not enough to used to measure the deformation field of nonrigid nonuniform biological tissues. Actually in SIFT and SURF methods, many interest points of initial image could not obtain the really corresponding points among the interest points in the deformed image, when the MR images are blurry and especially with nonuniform elastic deformation in the tissues. On the other hand, the match method such as the ratio of NN/SCN behaved not well in this case.

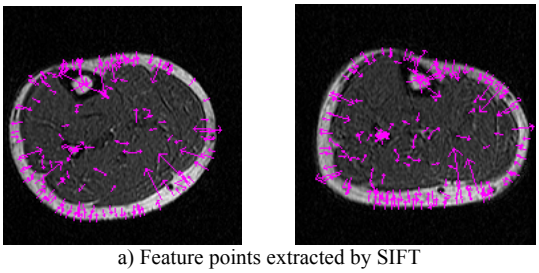

a) Feature points extracted by SIFT

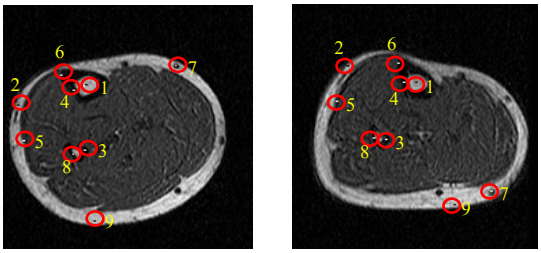

b) Matched points between initial and deformed MR image

Figure 6. The results of SIFT. Left: initial slice, Right: deformed slice.

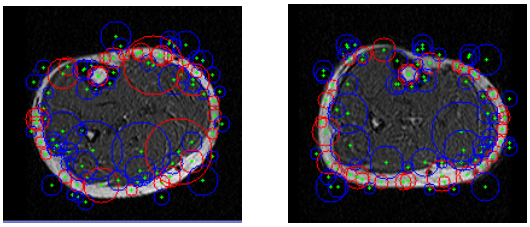

a) Feature points extracted by SURT

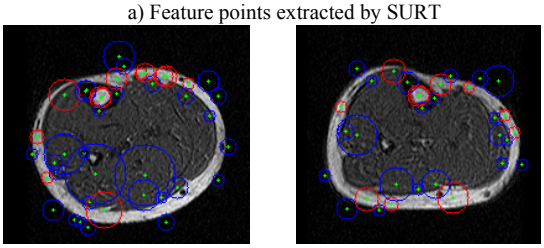

b) Matched points between initial and deformed MR image (41 pairs)

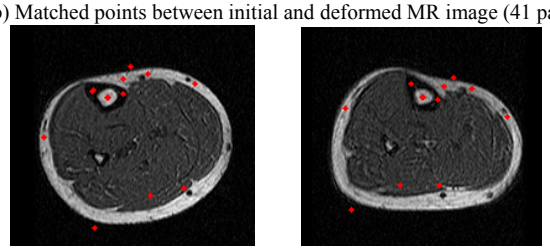

c) Correctly matched points (11 pairs)

Figure 7. The results of SURF

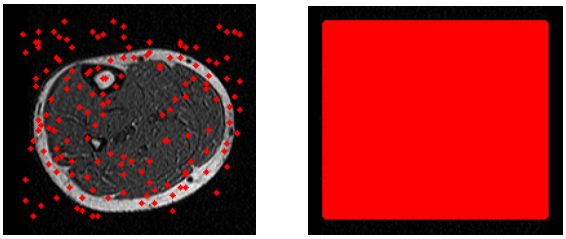

a) Feature points extracted by SURT

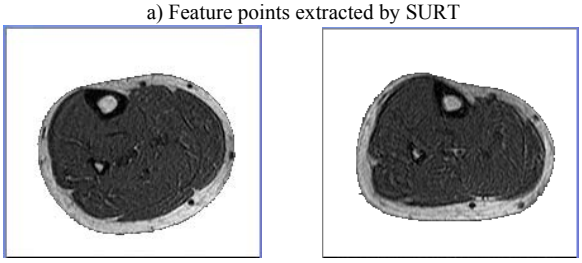

b) The results of background segmentation

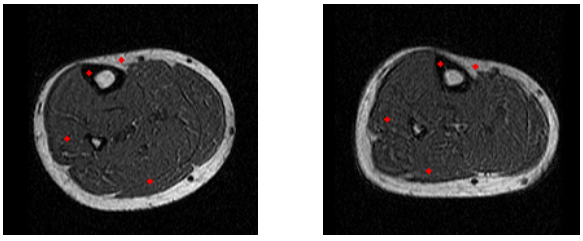

c) The matched points used for affine transformation evaluation

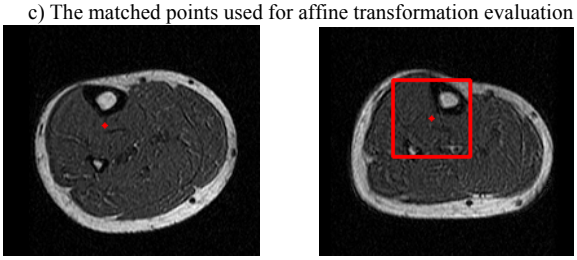

d) Searching region evaluated by affine transformation (radius = 30)

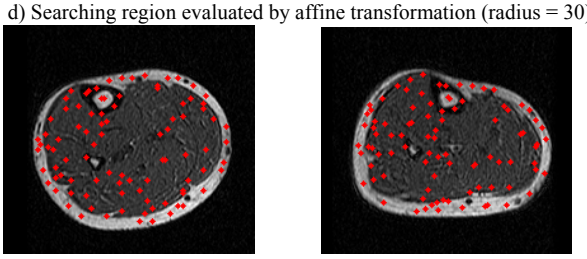

e) Matched points between initial and deformed MR image (93 pairs)

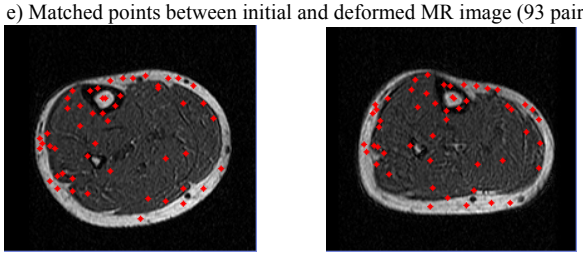

f) Correctly matched points (52 pairs)

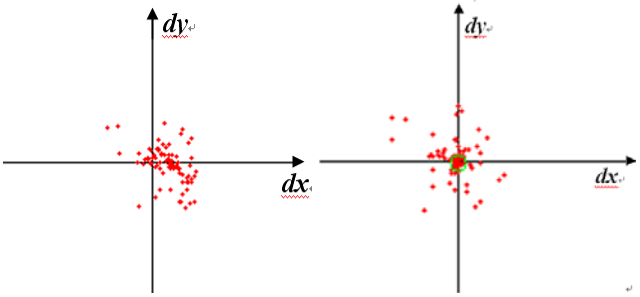

g) Coordinate difference points distribution h) The results of the clustering

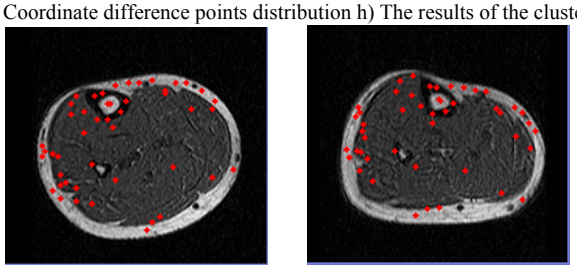

i) The matching points after clustering (48 pairs)

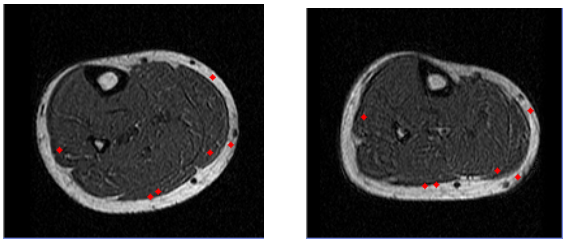

j) The wrong matched points are not eliminated by clustering (6 pairs)

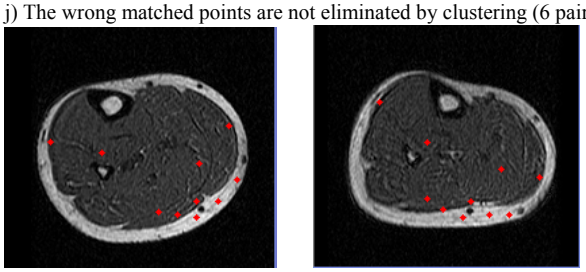

k) The correct matched points missed by clustering (10 pairs)

Figure 8. The results of SURF-SAC and Clustering

The experiment results are shown in Fig. 8. We used SURF-SAC to extract and match the feature points from the two MR images. In SAC method, we adopted spatial association corresponding relationship of two points in the neighbourhood of feature point, because when the number of the point increase the correct matched pairs decrease although the correctly match rate increase in this experiment. The matched points extracted by SURF-SAC are shown in Fig. 8-a). Fig. 8-b) showed the results of background segmentation, we used seed fill algorithm to segment the background, which avoided estimating the feature point in the background.

The evaluation of the affine transformation is based on the 4 pairs of matched points extracted by SURF (parameter T = 0.0004) and matched by NN/SCN with the ratio is of 0.65, which is shown in Fig. 8-c). The parameters of the affine transformation are $\theta = -14.19$, u = 13.869, v = 0.8974, $\Delta x = 44.73$, and $\Delta x = -13.68$. Given a feature point in the initial image, we only need to search the region centered with the corresponding point of affine transformation in the deformed image. The radius of the rectangle region equal to 30, and it reflects a pre-estimation of maximum deformation. Fig. 8-d) shows this step. By means of SURF-SAC, we obtained 93 pairs of matched points, and 52 pairs of points were correctly matched as shown in Fig. 8-e) and 10-f). The number of the correctly matched points was much more than that of SURF (or SIFT).

After this, for all initial points of the 93 matched pairs by SURF-SAC, we calculated the coordinate differences between the deformed points estimated by SURF-SAC with the corresponding points of affine transformation. Then we adopted clustering of the differences to eliminate the wrong matched points. The initial affine transformation model is estimated by the 4 points obtained by SURF, which is shown in Fig. 8-c). We set radius of the cluster circle equal to 5, and the difference points located in the cluster circle are used to calculate the affine transformation model again. Then the second affine transformation model is adopted to estimate the coordinate clustering. This process is repeated, and it can reduce the error introduced by the initial transformation model, which only adopted 4 points. In this experiment we set the iterative time equal to 10, more times are proved no much use to the results. The distribution of coordinate difference points is shown in Fig. 8-g), and results of clustering after 10 times iterative process is showed in Fig. 8-h), where the red points in the green circle denote to the correctly matched pairs.

There are 48 pairs of points are left after clustering, as shown in Fig. 8-i), and 6 wrong pairs are not eliminated by clustering as shown in Fig. 8-j). The correct rate reaches to 87.5%, especially in Fig. 8-j), the initial points and the wrong matched deformed points seem very likely to corresponding to each other although they are not the really corresponding pairs actually. Furthermore, there 10 correct pairs are missed by this means as shown in Fig. 8-k).

From the results of the experiments by our method, we can see that, SURF-SAC method can obtain more correctly matched point pairs between the initial and deformed MR images of the elastically deformed biological tissues than SURF (or SIFT) combined NN/SCN method. Furthermore, the coordinate difference clustering method can eliminate a large number of the wrong matched pairs.

VI. Conclusion

Current methods such as the transformation model estimation, physical model method, mutual information, and feature points combined with TIN cannot measure the nonrigid and nonuniform biological tissues deformation accurately. The extraction and matching of considerable number of feature points and elimination of the wrong matching pairs are the key issues of accurate elastic deformation field measurement.

SURF maybe the most outstanding method of feature point extraction, while unfortunately, when used in the deformation field measurement with the MR images of the nonrigid nonuniform biological tissues, the correctly matched points detected by SURF is too few to measure the local elastic deformation accurately.

In order to detecting more correct matching points between the initial and deformed MR images, the authors present Spatial Association Correspondence method combined SURF (SURF-SAC) to extract and match the feature points. SAC is based on the supposition that the neighboring pixels in the initial MR image would be probably neighboring in the deformed MR image. Further, clustering of the coordinate difference method is adopted to eliminate the wrong matched point pairs.

In the experiments, SIFT, SURF, and SURF-SAC are compared in the feature points extraction and matching of the MR images of the volunteer's calf. The experiment results show that SURF-SAC can detect more correctly matched points. For the elastic local deformation of nonrigid

nonuniform tissues, the accurate deformation is better to be measured by getting more correctly matched features. The other hand, the clustering of the difference between the deformed points matched by SURF-SAC with the corresponding points calculated by affine transformation can eliminate most of the wrong matched pairs.

While there are some limitations about our method, such as the computation cost is more than that of SIFT and SURF, and there are still some wrong matched pairs are not eliminated by clustering method also some correctly matched pairs are missed.

ACKNOWLEDGMENT

This work is partially supported by Prof. Shigerhiro Morikawa in Shiga University of Medical Science, Japan. The authors also gratefully acknowledge the helpful comments and the MR image data obtained.

REFERENCES

[1] P. L. Zhang, S. Hirai, K. Endo, and S. Morikawa, "Local deformation measurement of biological tissues based on feature tracking of 3D MR volumetric images," *IEEE/ICME International Conference on Complex Medical Engineering*, p. 711, 1982.

[2] P. L. Zhang, S. Hirai, and K. Endo, K., "A feature matching-based approach to deformation fields measurement from MR images of non-rigid object," *International Journal of Innovative Computing, Information and Control*, vol.4, pp. 1607–1625, 2008.

[3] Z. K. Wang, K. Namima, and S. Hirai, "Physical Parameter Identification of Uniform Rheological Deformation Based on FE Simulation," *Trans. Japanese Society for Medical and Biological Engineering*, Vol.47, No.1, pp. 1-6, Feb. 2009.

[4] Z. K. Wang, K. Namima, and S. Hirai, "Physical Parameter Identification of Rheological Object Based on Measurement of Deformation and Force," *IEEE International Conference on Robotics and Automation (ICRA 2009)*, *Kobe*, p. 1238, May. 2009.

[5] P. Kotsas, S. Malasiotis, M. G. Strintzis, et al. "A Fast and Accurate Method for Registration of MR Images of the Head", *International Journal on Medical Informatics*, vol. 52 (1-3), pp. 167-182, 1998.

[6] F. L. Bookstein. "Principal warps: thin-plate splines and decomposition of deformations", *IEEE Trans on Pattern Analysis and Machine Intelligence*, vol. 11(6), pp. 567-585, 1989.

[7] D. Rueckert, L. I. Sonoda, C. Hayes, et al. "Non-rigid registration using free-form deformations: Application to breast MR images", *IEEE Transactions on Medical Imaging*, vol. 18(8), pp. 712-721, 1999.

[8] M. Kass, A. Witkin, and D. TerzoPoulos, "Snake: active contour models," *International Journal of Computer Vision*, vol.1, pp. 321–331, 1987.

[9] V. Caselles, F. Catte, T. Coll, and F. Dibos, "A geometric model for active contours in image processing," *Numer. Math*., vol. 66, pp.1–31, 1993.

[10] Christensen G E, Rabbitt R D, Miller, et al. "Deformable templates using large deformation kinematics," IEEE Trans Image Process, 1996, 5: 1435-1447.

[11] J. P. Thirion. "Image matching as a diffusion process: an analogy with Maxwell's Demons", *Medical Image Analysis*, vol. 2, pp. 243-260, 1998.

[12] M. Ferrant. "Registration of 3-D intraoperative MRI images of the brain using a finite-element biomechanical model", *IEEE Trans. on Medical Imaging*, vol. 20(12), pp. 1384-1397, 2001.

[13] B. Likar, F. Pernus. "A Hierarchical Approach to Elastic Registration Based on Mutual Information", *Image and Vision Computing*, vol. 19(1-2), pp. 33-44, 2001.

[14] M. B. Skouson, Q. Guo, Z. P. Liang, "A Bound on Mutual Information for Image Registration", *IEEE Transactions on Medical Imaging*, vol. 20(8), pp. 843-846, 2001.

[15] T. Lindeberg, "Feature detection with automatic scale selection," *International Journal of Computer Vision*, vol. 30(2), pp. 79–116, 1998.

[16] D. Lowe, "Distinctive image features from scale-invariant keypoints, " *International Journal of Computer Vision*, vol. 60, pp. 91–110, 2004.

[17] K. Mikolajczyk, C. Schmid, "An affine invariant interest point detector," *The 7th European Conference on Computer Vision-Part I*, p.128, 2002.

[18] Y. Ke, and R. Sukthankar, "PCA-SIFT: A more distinctive representation for local image descriptors," *Computer Vision and Pattern Recognition*, vol. 2, pp. 506–513, 2004.

[19] C. Harris, and M. Stephens, "A combined corner and edge detector," *in Proceedings of the Alvey Vision Conference*, p.147, 1988.

[20] K. Mikolajczyk, and C. Schmid, "Indexing based on scale invariant interest points," *Proceedings of the 8th International Conference on Computer Vision, Vancouver, Canada*, p. 525. 2001.

[21] K. Mikolajczyk, and C. Schmid, "Scale and affine invariant interest point detectors." *International Journal of Computer Vision*, vol. 60, pp.63–86, 2004.

[22] K. Mikolajczyk, and C. Schmid, "A performance evaluation of local descriptors." *IEEE Transactions on Pattern Analysis and Machine Intelligence,* vol. 27, pp.1615–1630, 2005.

[23] L. M. J. Florack, Haar, B. M. t. Romeny, J. J. Koenderink, and M. A. Viergever, "General intensity transformations and differential invariants," *Journal of Mathematical Imaging and Vision*, vol. 4, pp. 171–187, 1994.

[24] F. Mindru, T. Tuytelaars, Gool, L.Van, and T. Moons, "Moment invariants for recognition under changing viewpoint and illumination," *Computer Vision and Image Understanding*, vol. 94, pp. 3–27, 2004.

[25] A. Baumberg, "Reliable feature matching across widely separated views," *IEEE Conference on Computer Vision and Pattern Recognition, Hilton Head Island, South Carolina, USA*, p. 774, 2000.

[26] H. Bay, T. Tuytelaars, and L. V. Gool, "SURF：Speeded Up Robust Features," *9th European Conference on Computer Vision, ECCV, Graz, Austria*, p.404, 2006.

[27] H. Bay, A. Ess, T. Tuytelaars, and L. V. Gool, "Speeded-up Robust Features (SURF)," *Computer Vision and Image Understanding*, vol. 110, pp. 346-359, March, 2008.